arXiv:0704.1993v1 [cond-mat.supr-con] 16 Apr 2007

# Competition between local and nonlocal dissipation effects in two-dimensional quantum Josephson junction arrays

T. P. Polak
*Consiglio Nazionale delle Ricerche - Istituto Nazionale per la Fisica della Materia,*
*Complesso Universitario Monte S. Angelo, 80126 Naples, Italy and*
*Istituto di Cibernetica "E.Caianiello" del CNR, Via Campi Flegrei 34, I-80078 Pozzuoli, Italy.*[*]

T. K. Kopeć
*Institute for Low Temperatures and Structure Research,*
*Polish Academy of Sciences, POB 1410, 50-950 Wroclaw 2, Poland*[†]

We discuss the local and nonlocal dissipation effects on the existence of the global phase coherence transitions in two dimensional Josephson-coupled junctions. The quantum phase transitions are also examined for various lattice geometries: square, triangular and honeycomb. The $T = 0$ superconductor-insulator phase transition is analyzed as a function of several control parameters which include self-capacitance and junction capacitance and both local and nonlocal dissipation effects. We found the critical value of the nonlocal dissipation parameter $\alpha_1$ depends on a geometry of the lattice. The critical value of the normal state conductance seems to be difficult to obtain experimentally if we take into consideration different damping mechanisms which are presented in real physical systems.

PACS numbers: 74.50.+r, 67.40.Db, 73.23.Hk

## I. INTRODUCTION

Macroscopic quantum effects in two-dimensional Josephson junction arrays (JJA's) have been extensively studied both theoretically[1,2,3,4,5,6,7] and experimentally[8,9,10] during the last years. The quantum nature of the phase of a superconducting order parameter is reflected in phase transitions in JJA's. In nondissipative JJA's the two main energy scales are set by the Josephson coupling $E_J$ between superconducting islands and the electrostatic energy $E_C$ arising from local deviations from charge neutrality. The ratio $E_C/E_J$ determines the relevance of the quantum fluctuations and when it increases above a critical value, the phase order is destroyed and the array turns into the insulator. For large capacitive coupling $E_C \gg E_J$ the system can be modeled by a renormalized classical two-dimensional ($2D$) $XY$ model. In the opposite limit, the energy cost for transferring charges between neighboring islands in the array is so high that charges tend to be localized. While the nature of the classical $2D$ $XY$ model is well understood, its quantum generalization still poses unsettled issues.

Modern fabrication techniques allow one to make arrays of ultrasmall superconducting islands separated by insulators. In such systems the important factor which has a profound impact on the ground state of the JJA's is dissipation caused by Ohmic resistors shunting the junctions[11,12,13] or quasiparticle tunneling through the junctions.[14,15,16] Despite several experiments with $2D$ JJA's[17,18] and superconducting granular films[19] existence of the dissipation driven transition and critical value of the normal state conductance is at least questionable.

Phase diagrams in quantum JJA's with both mechanisms of dissipation Ohmic and quasiparticle were studied theoretically by Zaikin.[20] Calculations done within the framework of the instanton technique reveal a zero temperature phase diagram with two dissipative phase transitions. The author claims there are regions on the phase diagram where disordered phase and the classical Josephson effect could take place. Cuccoli *et al.*[21] presented an analytical study based on the effective potential approach. They proposed a model in which two different relaxation times lead to the conductance matrix with resistive shunts to the ground and among islands. Despite of these accurate analytical studies the problem of a theoretical explanation of phase diagrams in JJA's in dissipative environment is still open.

Our previous theoretical work[22] in which the attention was focused on local dissipation effects, predicted the existence of the critical value of the dissipation parameter $\alpha = 2$ independent on geometry of a lattice and magnetic field. Other theoretical studies[11,12,23,24] suggest a rather broad range of the critical values of the dissipation parameter $\alpha = 0.5, 0.84, 1, 2$ which depends on the dimension of the system and mechanism of the dissipation. It seems that an unambiguous in experimental measurement of the critical value of the normal state conductance is elusive. Several groups[17,18,25,26,27,28,29] using different experimental techniques obtained various critical values of $\alpha = 0.5, 0.8, 1$. To explain these theoretical and experimental difficulties we propose a model in which local (caused by shunt resistors connecting the islands to a ground) and nonlocal (shunt resistors in parallel to the junctions) dissipation effects are considered.

The purpose of this paper is to investigate phase transitions at zero temperature in two-dimensional capacitively coupled superconducting arrays with emphasis on the competition of local $\alpha_0$ and nonlocal $\alpha_1$ dissipation effects. The detailed phase boundary crucially depends on the ratio of mutual to self-capacitances $C_1/C_0$ and specific planar geometry of the array.[4] Aware of that fact we consider capacitive matrix $C_{ij}$ within the range of parameters $C_1/C_0$ which can be adjusted to the experimental samples. We analyze phase diagrams for three different lattices: square (□), triangular (△) and honeycomb (H). We want to emphasize that our approximation cannot be used for analysis of the Berezinski-Kosterlitz-Thouless transitions since it is appropriate only for physical systems where long-range order appears.

The outline of the rest of the paper is the following: In Sec. II we define the model Hamiltonian, followed by its path integral formulation in terms of the dimensionality dependent nonmean-field like approach. In Sec III we present the zero-temperature phase diagram results for different JJA's geometries. Finally, in Sec. IV we discuss our results and their relevance to other theoretical and experimental works.

## II. MODEL

We consider a two-dimensional Josephson junction array with lattice sites $i$, characterized by superconducting phase $\phi_i$ in dissipative environment. The corresponding Euclidean action reads:

$$\mathcal{S} = \mathcal{S}_{\rm C} + \mathcal{S}_{\rm J} + \mathcal{S}_{\rm D}, \tag{1}$$

where

$$\begin{aligned}
\mathcal{S}_{\rm C} &= \frac{1}{8e^2}\sum_{i,j}\int_0^\beta d\tau \left(\frac{\partial\phi_i}{\partial\tau}\right) C_{ij} \left(\frac{\partial\phi_j}{\partial\tau}\right), \\
\mathcal{S}_{\rm J} &= \sum_{\langle i,j\rangle}\int_0^\beta d\tau J_{ij}\left\{1-\cos\left[\phi_i(\tau)-\phi_j(\tau)\right]\right\}, \\
\mathcal{S}_{\rm D} &= \frac{1}{2}\sum_{i,j}\int_0^\beta d\tau d\tau' \alpha_{ij}(\tau-\tau')\left[\phi_i(\tau)-\phi_j(\tau')\right]^2
\end{aligned} \tag{2}$$

and $\tau$ is the Matsubara's imaginary time ($0 \leq \tau \leq 1/k_{\rm B}T \equiv \beta$); $T$ is temperature and $k_{\rm B}$ the Boltzmann constant ($\hbar = 1$). The first part of the action (2) defines the electrostatic energy where $C_{ij}$ is the capacitance matrix which is a geometric property of the array. This matrix is usually approximated as a diagonal (self-capacitance $C_0$) and a mutual one $C_1$ between nearest neighbors. We can write a general expression for the $C_{ij}$ in the following form:

$$C_{ij} = \begin{cases} C_0 + zC_1 & \text{for} \quad i=j \\ -C_1 & \text{for nearest neighbors} \end{cases} \tag{3}$$

which holds for periodic structures in any dimension; $z$ is coordination number of the network. The second term is the Josephson energy $E_J$ ($J_{ij} \equiv E_J$ for $|i-j| = |d|$ and zero otherwise). The vector $d$ forms a set of $z$ lattice translation vectors, connecting a given site to its nearest neighbors. The Fourier transformed wave-vector dependent Josephson couplings $J_{\mathbf{k}}$ are different for various lattices. The third part of the action $\mathcal{S}_{\rm D}$ describes the dissipation effects and $\alpha_{ij}(\tau-\tau')$ is a dissipation matrix. We choose two independent damping mechanisms, the on-site and the nearest-neighbor, because usually, the damping is described in terms of shunt resistors $R_0$ connecting the islands to a ground and shunt resistors in parallel to the junctions related to $R_1$. We can write dissipation matrix similar to Eq. (3) in a more closed form:

$$\alpha_{ij} = (\alpha_0 + z\alpha_1)\,\delta_{ij} - \alpha_1 \sum_d \delta_{i,j+d} \tag{4}$$

with the vector $d$ running over nearest neighboring islands. The dimensionless parameters

$$\alpha_0 = \frac{R_Q}{R_0}, \qquad \alpha_1 = \frac{R_Q}{R_1}. \tag{5}$$

describe strength of the local and nonlocal dissipation respectively, where $R_Q = 1/4e^2$ is quantum resistance.

### A. Method

Most of existing analytical works on quantum JJA's have employed different kinds of mean-field-like approximations which are not reliable for treatment spatial and temporal quantum phase fluctuations. The model in Eq. 2 encodes the phase fluctuation algebra given by Euclidean group $E_2$ defined by commutation relations between particle $L_i$ and phase $P_j$ operators,

$$\begin{aligned}
P_j &= e^{i\phi_j}, \\
[L_i, P_j] &= -P_i\delta_{ij}, \\
\left[L_i, P_j^\dagger\right] &= P_i^\dagger\delta_{ij}, \\
[P_i, P_j] &= 0,
\end{aligned} \tag{6}$$

with the conserved quantity (invariant of the $E_2$ algebra)

$$P_iP_i^\dagger \equiv P_{xi}^2 + P_{yi}^2 = 1. \tag{7}$$

The proper theoretical treatment of the quantum JJA's must maintain the constraint in Eq. 7. A formulation of the problem in terms of the spherical model initiated by Kopeć and José[31] leads us to introduce the auxiliary complex field $\psi_i$ which replaces the original operator $P_i$. Furthermore, relaxing the original "rigid" constraint and imposing the weaker spherical condition:

$$\sum_i P_iP_i^\dagger = N. \tag{8}$$

where $N$ is the number of lattice sites, allows us to implementation the spherical constraint:

$$\begin{aligned}\mathcal{Z} &= \int [\mathcal{D}\psi]\,\delta\left(\sum_i |\psi_i|^2 - N\right) e^{-\mathcal{S}_{\rm J}[\psi]} \\ &\times \int [\mathcal{D}\phi]\, e^{-\mathcal{S}_{\rm C+D}[\phi]} \prod_i \delta\left[\mathrm{Re}\psi_i - P_{xi}(\phi)\right] \\ &\times \delta\left[\mathrm{Im}\psi_i - P_{yi}(\phi)\right].\end{aligned} \tag{9}$$

where $[\mathcal{D}\psi] = \prod_i \mathcal{D}\psi_i \mathcal{D}\psi_j^*$ and $[\mathcal{D}\phi] = \prod_i \mathcal{D}\phi_i$. It is convenient to employ the functional Fourier representation of the $\delta$ functional to enforce the spherical constraint in Eq. (8):

$$\delta\left[x(\tau)\right] = \int_{-i\infty}^{+i\infty} \left[\frac{\mathcal{D}\lambda}{2\pi i}\right] e^{\int_0^\beta d\tau \lambda(\tau) x(\tau)}, \tag{10}$$

which introduces the Lagrange multiplier $\lambda(\tau)$ thus adding a quadratic term (in $\psi$ field) to the action in Eq. (2). The evaluation of the effective action in terms of the $\psi$ to second order in $\psi_i$ gives the partition function of the quantum spherical model (QSM)

$$\mathcal{Z}_{\rm QSM} = \int [\mathcal{D}\psi]\,\delta\left(\sum_i |\psi_i|^2 - N\right) e^{-\mathcal{S}[\psi]} \tag{11}$$

where the effective action reads:

$$\begin{aligned}\mathcal{S}[\psi] &= \sum_{\langle i,j\rangle} \int_0^\beta d\tau d\tau' \left\{\left[J_{ij}(\tau)\,\delta(\tau-\tau')\right.\right. \\ &+ \left.\mathcal{W}_{ij}^{-1}(\tau,\tau') - \lambda(\tau)\,\delta_{ij}\delta(\tau-\tau')\right]\psi_i\psi_j^* \\ &+ \left. N\lambda(\tau)\,\delta(\tau-\tau')\right\}.\end{aligned} \tag{12}$$

Furthermore,

$$\mathcal{W}_{ij}(\tau,\tau') = \frac{\delta_{ij}}{\mathcal{Z}_0} \int [\mathcal{D}\phi]\, e^{i\left[\phi_i(\tau)-\phi_j(\tau')\right]} e^{-\mathcal{S}_{\rm C+D}[\phi]}, \tag{13}$$

is the phase-phase correlation function with statistical sum

$$\mathcal{Z}_0 = \int [\mathcal{D}\phi]\, e^{-\mathcal{S}_{\rm C+D}[\phi]}, \tag{14}$$

where action $\mathcal{S}_{\rm C+D}[\phi]$ is just a sum of electrostatic and dissipative terms in Eq. (2). After introducing the Fourier transform of the field

$$\phi_i(\tau) = \frac{1}{N\beta} \sum_{\mathbf{k}} \sum_{n=-\infty}^{+\infty} \phi_{\mathbf{k},n} e^{-i(\omega_n\tau - \mathbf{k}\mathbf{r}_i)} \tag{15}$$

with $\omega_n = 2\pi n/\beta$, $(n = 0, \pm1, \pm2, ...)$ being the Bose Matsubara frequencies. From Eq. (13) the phase-phase correlation function reads:

$$\mathcal{W}(\tau,\tau') = \exp\left\{-\frac{1}{\beta}\sum_{n\neq 0} \frac{1-\cos\left[\omega_n(\tau-\tau')\right]}{\frac{1}{8E_C}\omega_n^2 + \frac{\alpha}{2\pi}\frac{J_{\mathbf{k}}}{E_J}|\omega_n|}\right\}. \tag{16}$$

The charging energy parameter entering Eq. (16) is

$$E_C = \frac{1}{2}e^2\left[\mathbf{C}^{-1}\right]_{ii} = \frac{e^2}{\pi\left(C_0+4C_1\right)}\mathbf{K}\left(\frac{4C_1}{C_0+4C_1}\right) \tag{17}$$

where $\mathbf{K}(x)$ is the elliptic integral of the first kind[32]. Furthermore we introduce quantities $E_0 = e^2/2C_0$ and $E_1 = e^2/2C_1$ related to the island and junction capacitances.

The dissipative parameter $\alpha$ and may be explicitly written as

$$\alpha^{-1} = \lim_{N\to\infty}\frac{1}{N}\sum_{\mathbf{k}}\frac{1}{\alpha_0 + z\alpha_1 - 2\alpha_1\mathcal{E}_{\mathbf{k}}} \tag{18}$$

where $\mathcal{E}_{\mathbf{k}}$ is a dispersion and has different form for various lattices. In the present paper we consider three different geometries of the lattice: square (□), triangular (△) and honeycomb (H):

$$\begin{aligned}\mathcal{E}_{\mathbf{k}}^{\square} &= \cos k_x + \cos k_y, \\ \mathcal{E}_{\mathbf{k}}^{\triangle} &= \cos k_x + 2\cos\left(\frac{k_x}{2}\right)\cos\left(\frac{\sqrt{3}}{2}k_y\right), \\ \mathcal{E}_{\mathbf{k}}^{\rm H} &= \sqrt{\frac{1}{2}\left(\frac{3}{2}+\mathcal{E}_{\mathbf{k}}^{\triangle}\right)}.\end{aligned} \tag{19}$$

with the lattice spacing set to 1. The results of the sum over wave vectors in Eq. 18 are placed in Appendix B. Finally, for small frequencies, $\alpha_0 \leq 2$ and $\alpha_1 \leq 1$ the inverse of correlation function (16) becomes:

$$\mathcal{W}^{-1}(\omega_n) = \left\{\begin{array}{c} \frac{1}{8E_C}\omega_n^2 + \frac{\alpha}{2\pi}\frac{J_{\mathbf{k}}}{E_J}|\omega_n| \quad \text{for} \quad \omega_n \neq 0 \\ 0 \quad \text{otherwise}\end{array}\right. \tag{20}$$

In order to determine the Lagrange multiplayer $\lambda$ we observe that in the thermodynamic limit $(N\to\infty)$ the steepest descent method becomes exact. The condition the integrand in Eq. (11) has a saddle point $\lambda(\tau) = \lambda_0$, leads to an implicit equation for $\lambda_0$:

$$1 = \frac{1}{\beta N}\sum_{\mathbf{k}}\sum_{n\neq 0} G(\mathbf{k},\omega_n), \tag{21}$$

where

$$G^{-1}(\mathbf{k},\omega_n) = \lambda_0 - J_{\mathbf{k}} + \frac{1}{8E_C}\omega_n^2 + \frac{\alpha}{2\pi}\frac{J_{\mathbf{k}}}{E_J}|\omega_n|. \tag{22}$$

The emergence of the critical point in the model is signaled by the condition

$$G^{-1}(\mathbf{k}=0,\omega_n=0) \equiv \lambda_0 - J_0 = 0 \tag{23}$$

which fixes the saddle point of the Lagrange multiplier $\lambda_0$ within the ordered phase $\lambda_0 = J_0$.

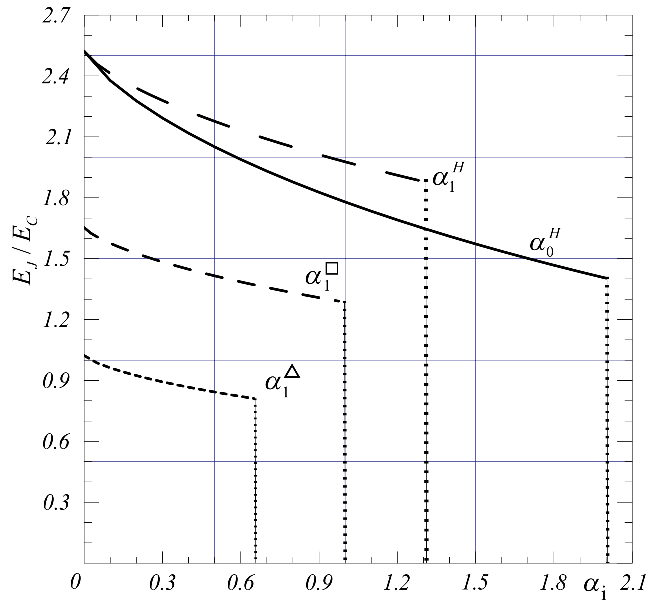

Figure 1: Zero-temperature phase diagram for the total charging energy $E_J/E_C$ vs parameter of dissipation $\alpha_i$ ($i=1$ if $\alpha_0=0$ and $i=0$ if $\alpha_1=0$) for triangular ($\triangle$; $\alpha_1^{\rm crit}=2/3$), square ($\square$; $\alpha_1^{\rm crit}=1$) and honeycomb ($H$; $\alpha_1^{\rm crit}=4/3$) lattice. Insulating (superconducting) state is below (above) the curves.

## III. PHASE DIAGRAMS

A Fourier transform of the Green function in Eq. (22) enables one to write the spherical constraint (21) explicitly as:

$$1=\frac{1}{\beta}\int_{-\infty}^{+\infty}d\xi\sum_{n\neq 0}\frac{\rho\left(\xi\right)}{\lambda-\xi E_J+\frac{1}{8E_C}\omega_n^2+\frac{\alpha}{2\pi}\xi\left|\omega_n\right|}. \quad (24)$$

where

$$\rho\left(\xi\right)=\frac{1}{N}\sum_{\mathbf{k}}\delta\left[\xi-\frac{J_{\mathbf{k}}}{E_J}\right] \quad (25)$$

is the density of states. We can easily see that solution of the model requires the knowledge of the DOS for a specific lattice with the superimposition of the self-consistency condition for the critical line in Eq. (24). A Josephson-junction array network is characterized for different lattices by the nearest-neighbor Josephson coupling $E_J$ with the following wave-vector dependence

$$\begin{aligned} J_{\mathbf{k}}^{\square} &= E_J\mathcal{E}_{\mathbf{k}}^{\square}\\ J_{\mathbf{k}}^{\triangle} &= E_J\mathcal{E}_{\mathbf{k}}^{\triangle}\\ J_{\mathbf{k}}^{\rm H} &= E_J\mathcal{E}_{\mathbf{k}}^{\rm H} \end{aligned} \quad (26)$$

where $\mathcal{E}_{\mathbf{k}}$'s are given by Eq. 19. The Fourier transform of the capacitance (dissipative) matrices for a triangular and honeycomb lattice[4] can be also found in Appendix C.

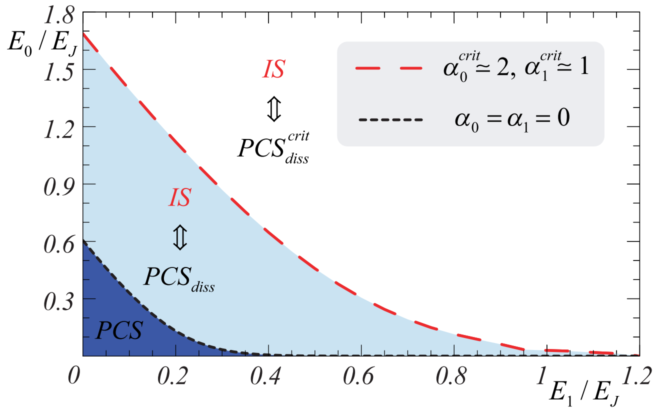

Figure 2: Zero-temperature phase diagram for square 2D JJA's with self $C_0=e^2/2E_0$ and mutual $C_1=e^2/2E_1$ capacitance (Eq. 17) for two values of local and nonlocal dissipation parameter $\alpha_0=\alpha_1=0$ and $\alpha_0=2$ and $\alpha_1=1$ (see Appendix). We can distinguish three areas: phase coherent state ($PCS$) where phases in the islands are well defined. Insulating state ($IS$) which could be driven to the phase coherent state by effects of the dissipation ($PCS_{diss}$). Finally, insulating state, where superconducting phase is perturbed by strong zero point quantum fluctuations due to Coulomb blockade that localizes charge carries to the islands. However system can be driven to the phase coherent state ($PCS_{diss}^{crit}$) but only by critical values of the dissipation parameters ($\alpha_0^{\rm crit}\simeq 2$ and $\alpha_1^{\rm crit}\simeq 1$).

By substituting the value of $\lambda_0=J_{\rm max}$ where $J_{\rm max}$ denotes maximum value of the spectrum $J_{\mathbf{k}}$, and after performing the summation over Matsubara frequencies, in $T\to 0$ limit we obtain the following result:

$$\begin{aligned} 1 &= \frac{1}{\pi}\int_{-\infty}^{+\infty}d\xi\frac{\rho\left(\xi\right)}{\sqrt{\left(\frac{\alpha}{2\pi}\xi\right)^2-\frac{J_{\rm max}-\xi E_J}{2E_C}}}\\ &\times\ln\left[\frac{\frac{\alpha}{2\pi}\xi+\sqrt{\left(\frac{\alpha}{2\pi}\xi\right)^2-\frac{J_{\rm max}-\xi E_J}{2E_C}}}{\frac{\alpha}{2\pi}\xi-\sqrt{\left(\frac{\alpha}{2\pi}\xi\right)^2-\frac{J_{\rm max}-\xi E_J}{2E_C}}}\right]. \end{aligned} \quad (27)$$

The critical values of the nonlocal dissipation parameters have a source in low temperature properties of the JJA's correlation function in dissipative environment (Appendix A). The dependence of the critical value $\alpha_1$ depicted in Fig. 1 is a direct result of the divergence this phase-phase correlator. The Fig. 2 and Fig. 3 point out the big difference in values of the self $C_0$ and mutual $C_1$ capacitance and competition between various dissipation mechanisms have a severe impact on phase diagrams. In typical real situations mutual capacitance can be at least two orders of magnitude larger than the self-capacitance what indicates the samples are placed very close to $E_1/E_J$ axis in Fig. 2.

JJA's devoid of dissipation effects can be in two phases: insulator phase ($IS$) and phase coherent state ($PCS$). However coupling system to the environment we are able

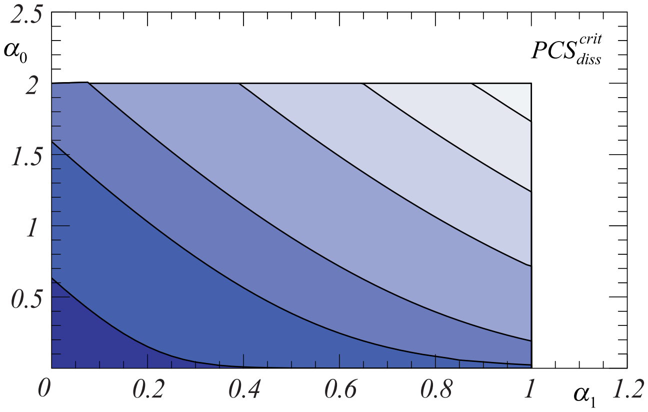

Figure 3: Zero-temperature phase diagram for square 2D JJA's in space of local $\alpha_0$ and nonlocal $\alpha_1$ dissipation parameters for several values of the ratio $C_1/C_0$. From the top $C_1/C_0 = 1.25, 1.67, 2.5, 5, 10, 50$. Insulating (superconducting) state below (above) the curves.

to drive arrays into $PCS$ even if localization of the charge carriers due to Coulomb blockade is strong and dominates properties of the system. Furthermore for each geometry of the lattice there are critical values of the dissipation parameters that lead arrays to situation (Fig. 2) where phases in the islands are well defined and quantum fluctuations do not perturb a superconducting phase - region describe as $PCS^{crit}_{diss}$. Notwithstanding between these two boundary situations there is a region on the phase diagram in Fig. 2 where concrete situation depends on the values of the parameters. In this area $PCS_{diss}$ system can be driven to the $PCS$ but coupling to the environment does not have to be so strong as in $PCS^{crit}_{diss}$ case.

## IV. RESULTS

Until now only three papers considered effects with both mechanisms of the dissipation.[11,20,21] The most interesting is Cuccoli's work where authors introduced the full conductance matrix for triangular and square lattices. It seems their results improve the quantitative accuracy; nevertheless problem of the theoretical explanation of the phase diagram of JJA's in dissipative environments is thus open.

A model of an ordered array of resistively shunted Josephson junctions was also considered by Chakravarty *et. al.*[11] and simplified at several points. They assumed that capacitance matrix is diagonal $C_{ij} = C\delta_{ij}$. The authors claim the results do not depend sensitively on detailed form of $C_{ij}$. Moreover the matrix $\alpha_{ij} = h/4e^2R_{ij}$ where $R_{ij}$ is the shunting resistance between grains $i$ and $j$ is reduced to the form in which the information about the geometry of the lattice is not included. The obtained zero-temperature phase diagram reveals the fact that the critical value of the dissipation exists and is proportional to the inverse of the dimension of the system which gives us critical value $\alpha = 1/2$ for a square lattice, but especially at low temperatures, variational methods are not precise enough to perceive such a subtle transition.

In our model the critical value of the nonlocal dissipation parameter $\alpha_1$ behaves similarly. It depends on the maximum value of the $J_{\mathbf{k}}$ spectrum. Because $J_{\mathbf{k}}$ exhibits different characters for various lattices hence we could observe phenomenon such as nonmonotonic dependence of the critical value of the nonlocal dissipation parameter for various geometries of the array (see Fig. 1). When we assume diagonal form $\alpha_{ij} = \alpha_0\delta_{ij}$ then obviously our results will not change when we change the geometry of the lattice simply because the shunt resistors connecting the islands to ground are the same for each island. On the other hand if we take into consideration that $\alpha_0 = 0$ and only $\alpha_1$ is present, the situation changes because now values of the dissipative matrix strongly depend on the $J_{\mathbf{k}}$ spectrum which indicates various values of the matrix $\alpha_{ij}$ depend on the geometry of the structure. This case is present in arrays with shunt resistors in parallel to the junctions.

A standard way to study models with only diagonal charging energies $C_{ij} = C\delta_{ij}$ corresponds to a complete absence of screening by the other islands in the array.[33] Notice the mutual capacitance can be at least two orders of magnitude larger than the self-capacitance[9] $C_1 \simeq 10^2 C_0$. We propose a more realistic model in which both self and mutual capacitances are nonzero. To see how significant this consideration is we shall analyze Fig. 3. If we assume, that $C_1/C_0 \simeq 50$ (see the lowermost line in Fig. 3) we can see the critical values of the dissipation parameters change dramatically from local $\alpha_0 = 2$ and nonlocal $\alpha_1 = 1$ (Appendix A) obtained for fewer realistic cases $C_1/C_0 = 1$ in which both of the capacitances are comparable. In the limit $(C_1 \neq 0, C_0 = 0)$ the lattice model is equivalent to the Coulomb gas model with critical properties not fully understood at present. However we have to emphasize that the range of the Coulomb matrix becomes infinite when $C_0$ is set equal to zero. The phase boundary in Fig. 3 shift downward with increasing ratio $C_1/C_0$ because lower value of the Coulomb interaction between nearest neighbors reduces strong quantum phase fluctuations and in consequence we observe a growth of long-range phase coherence.

Yagi *et al.*[25] experimented with the superconductor-insulator transition in two-dimensional network of Josephson junctions in detail by varying the junctions-area. It was observed the critical tunneling resistance exhibited significant junction area dependence. The low-temperature behavior of the total charging energy $E_J/E_C$ as a function $R_Q/R_n$, where $R_n$ is the tunneling resistance exhibits the same behavior as the curve obtained from our theory for square lattices (see Figure 1) in the absence of the local dissipation effects $\alpha_0 = 0$. The observed phase boundary, which is bending downward, and the critical value of the nonlocal dissipation parameter $\alpha_1^{\mathrm{crit}} = 1$ is in excellent accordance with our results.

In order to investigate the effects of quantum fluctuations and dissipation in JJA's, another group[18] made two-dimensional arrays of small junctions with various $E_J/E_C$ and resistors which caused dissipation effects. The value of $E_J$ was controlled by varying the tunnel resistance. Each island was connected to the neighboring ones by a shunt resistor as well as the tunnel junction. The resistance of the shunt resistors was tuned by varying their length. Ground states of $2D$ Josephson array in $E_J/E_C$-$R_Q/R_s$ parameters space reveal the same behavior as previous experimental results but there is a difference in critical value of the $R_Q/R_s \simeq 0.5$ which also differs from value $\alpha_1^{\mathrm{crit}}$ obtained in this paper. These discrepancies between experiments can be explained in the framework of our model by taking into account different value of the ratio junction-to-self capacitances which reduces the critical value of the $R_Q/R_s$ and considering that not only nonlocal dissipation mechanism is present $\alpha_0 \neq 0$ we can obtain $R_Q/R_s \simeq 0.5$ value (see Figure 3). Real numbers strongly depend on the properties of the junctions used in experiments.

## V. SUMMARY

We have calculated quantum phase diagrams of two-dimensional Josephson junction arrays using the spherical model approximation. The calculations were performed for systems using experimentally attainable geometries for the arrays such us square, triangular and honeycomb. The ground state of the Josephson coupled array with a triangular lattice appears to be most stable against the Coulomb effects. This geometry is also the case in which the global coherent state emerged when the value of the nonlocal dissipation parameter $\alpha_1$ is the lowest. In JJA's we can observe the phase coherence transition which is caused by electrostatic and dissipative effects. The detailed phase diagrams crucially depend on the ratio junction-to-self capacitances, $C_1/C_0$ and both dissipation mechanism have a big impact on phase boundaries. The nondiagonal terms in capacitive and dissipative matrices can change the phase diagrams of the system drastically . It is necessary to take them into considerations when we have different sources of dissipation such us shunt resistors connecting the islands to a ground and shunt resistors in parallel to the junctions. The experimental observation of an universal resistance threshold for the onset of the global coherent state seems possible, but appears to be difficult.

### Acknowledgments

One of the authors wants to thank Dr. Ettore Sarnelli for carefully reading manuscript and fruitful discussions. This work was supported by the TRN "DeQUACS" and some parts of it were done in Max-Planck-Institut für Physik komplexer Systeme, Nöthnitzer Straße 38, 01187 Dresden, Germany.

| DOS | $\triangle$ | H | $\square$ |
|---|---|---|---|
| $J_{\max}/E_J$ | 3 | $\frac{3}{2}$ | 2 |

Table I: Maximum values of the spectrum $J(k)$ for three different geometries of the lattices: triangular ($\triangle$), honeycomb (H) and square ($\square$)

## Appendix A: SOME PROPERTIES OF THE CORRELATOR

Assume that $\alpha_0 = 0$ we write expression for the phase-phase correlation function (similar to equation used in a previous calculations[22] but modified by dissipative matrix) in form:

$$\mathcal{W}(\tau) = \exp\left\{ -\frac{1}{\beta} \sum_{n\neq 0} \frac{1-\cos(\omega_n \tau)}{\frac{1}{8E_C}\omega_n^2 + \frac{\alpha_1}{2\pi}\frac{J_{\mathbf{k}}}{E_J}|\omega_n|} \right\}. \tag{A1}$$

It is easy to see the sum over $\omega_n$ is symmetric when we change $\omega_n \to -\omega_n$. The key to obtain the solution is a calculation the sum or the integral under the exponent in Eq. (A1). Because we are going to investigate low-temperature properties of the correlation function we could write $\frac{1}{\beta}\sum_{\omega_n} \to \frac{1}{2\pi}\int_{-\infty}^{+\infty} d\omega$. In that case (getting rid of abs) for large value $\tau$ we write

$$\begin{aligned}\mathcal{W}(\tau) &= \exp\left[ -\frac{1}{\pi}\int_0^{+\infty} d\omega \frac{1-\cos(\tau\omega)}{\frac{1}{8E_C}\omega^2 + \frac{\alpha_1}{2\pi}\frac{J_{\mathbf{k}}}{E_J}\omega} \right] \\ &\simeq \exp\left( -\frac{2\gamma E_J}{\alpha_1 J_{\mathbf{k}}} \right) \left( \frac{\alpha_1 J_{\mathbf{k}} E_C}{4\pi E_J} |\tau| \right)^{2E_J/\alpha_1 J_{\mathbf{k}}} \end{aligned} \tag{A2}$$

where $\gamma = 0.57721$ is the Euler-Mascheroni constant. Finally, after Fourier transform we see that correlator $\mathcal{W}^{-1}(\omega_m) \sim |\omega_m|^{2E_J/\alpha_1 J_{\max} - 1}$ at zero temperature diverges for $\alpha_1 \geq 2E_J/J_{\max}$. Quantity $J_{\max}/E_J$ means the maximum value of the $J_{\mathbf{k}}$ which differs for various lattices (see Table I).

## Appendix B: DISSIPATION PARAMETER FOR CONSIDERED LATTICES

In this appendix we give the explicit formulas for the dissipation parameter discussed in Sec. II and III.

### 1. Square lattice

$$\alpha_{\square}^{-1} = \frac{2}{\pi(\alpha_0 + 4\alpha_1)} \mathbf{K}\left( \frac{4\alpha_1}{\alpha_0 + 4\alpha_1} \right) \tag{B1}$$

where

$$\mathbf{K}\left(x\right)=\int_0^{\pi/2}\frac{d\phi}{\sqrt{1-x^2\sin^2\phi}}, \tag{B2}$$

is the elliptic integral of the first kind[32] and the unit step function is defined by:

$$\Theta\left(x\right)=\begin{cases}1 & \text{for } x>0\\ 0 & \text{for } x\le 0\end{cases}. \tag{B3}$$

For small values of the $\alpha_1$ we can write dissipation parameter for square lattice as:

$$\alpha_{\Box}=\alpha_0+3\alpha_1-\frac{5}{4}\frac{\alpha_1}{\alpha_0}+\frac{9}{4}\frac{\alpha_1^3}{\alpha_0^2}+\mathcal{O}\left(\alpha_1^4\right), \tag{B4}$$

for large values values of the $\alpha_1$:

$$\alpha_{\Box}=\frac{4\pi\alpha_1}{\ln\left(\frac{64\alpha_1}{\alpha_0}\right)}+\frac{1}{4}\pi\alpha_0\left[3-\frac{2}{\ln\left(\frac{64\alpha_1}{\alpha_0}\right)}\right]+\mathcal{O}\left(\frac{1}{\alpha_1}\right). \tag{B5}$$

### 2. Triangular lattice

$$\alpha_{\triangle}^{-1}=\frac{1}{\pi\sqrt{3}}\frac{g}{\alpha_1}\mathbf{K}\left(\kappa\right) \tag{B6}$$

where

$$g=\frac{8}{\left[\left(2t+3\right)^{1/2}-1\right]^{3/2}\left[\left(2t+3\right)^{1/2}+3\right]^{1/2}} \tag{B7}$$

$$\kappa=\frac{4\left(2t+3\right)^{1/4}}{\left[\left(2t+3\right)^{1/2}-1\right]^{3/2}\left[\left(2t+3\right)^{1/2}+3\right]^{1/2}} \tag{B8}$$

with $t=\left(\alpha_0+6\alpha_1\right)/2\alpha_1$.

### 3. Honeycomb lattice

$$\alpha_{\mathrm{H}}^{-1}=\frac{1}{\pi\sqrt{3}}\frac{g}{\alpha_1}\frac{\alpha_0+3\alpha_1}{\alpha_1}\mathbf{K}\left(\kappa\right) \tag{B9}$$

where

$$g=\frac{8}{\left(2t-1\right)^{3/2}\left(2t+3\right)^{1/2}} \tag{B10}$$

$$\kappa=\frac{4^{1/4}\left(2t\right)^{1/2}}{\left(2t-1\right)^{3/2}\left(2t+3\right)^{1/2}} \tag{B11}$$

with $t=\left(\alpha_0+3\alpha_1\right)/2\alpha_1$.

## Appendix C: DOS FOR CONSIDERED LATTICES

In this appendix we give the explicit formulas for the density of states discussed in Sec. II and III.

### 1. Square lattice

$$\rho^{\Box}\left(\xi\right)=\frac{1}{\pi^2}\mathbf{K}\left(\sqrt{1-\left(\frac{\xi}{2}\right)^2}\right)\Theta\left(1-\left|\frac{\xi}{2}\right|\right), \tag{C1}$$

### 2. Triangular lattice

$$\rho^{\triangle}\left(\xi\right)=\frac{2}{\pi^2\sqrt{\kappa_0}}\mathbf{K}\left(\sqrt{\frac{\kappa_1}{\kappa_0}}\right)\left[\Theta\left(\xi+\frac{3}{2}\right)-\Theta\left(\xi-3\right)\right], \tag{C2}$$

where

$$\begin{aligned}\kappa_0 &= \left(3+2\sqrt{3+2\xi}-\xi^2\right)\left[\Theta\left(\xi+\frac{3}{2}\right)-\Theta\left(\xi+1\right)\right]\\ &+ 4\sqrt{3+2\xi}\left[\Theta\left(\xi+1\right)-\Theta\left(\xi-3\right)\right],\end{aligned} \tag{C3}$$

$$\begin{aligned}\kappa_1 &= 4\sqrt{3+2\xi}\left[\Theta\left(\xi+\frac{3}{2}\right)-\Theta\left(\xi+1\right)\right]\\ &+ \left(3+2\sqrt{3+2\xi}-\xi^2\right)\left[\Theta\left(\xi+1\right)-\Theta\left(\xi-3\right)\right]\end{aligned} \tag{C4}$$

### 3. Honeycomb lattice

$$\rho^{\mathrm{H}}\left(\xi\right)=4\left|\xi\right|\rho^{\triangle}\left(3-4\xi^2\right). \tag{C5}$$

---

[*] Electronic address: polak@fisica.cib.na.cnr.it

[†] Electronic address: kopec@int.pan.wroc.pl

[1] E. Šimánek, Solid State Commun. **31**, 419 (1979).

[2] S. Doniach, Phys. Rev. B **24**, 5063 (1981).

[3] D. M. Wood and D. Stroud, Phys. Rev. B **25**, 1600 (1982).

[4] T. K. Kopeć and J. V. José, Phys. Rev. B **63**, 064504 (2001).

[5] J. V. José, Phys. Rev. B **29**, R2836 (1984); L. Jacobs, J. V. José and M. A. Novotny, Phys. Rev. Lett. **53**, 2177 (1984).

[6] T. K. Kopeć and T. P. Polak, Phys. Rev. B **66**, 094517 (2002).

[7] V. Ambegaokar, U. Eckern and G. Schön, Phys. Rev. Lett. **48**, 1745 (1982).

[8] R. F. Voss and R. A. Webb, Phys. Rev B **25**, R3446 (1982).

[9] B. J. van Wees, H. S. J. van der Zant, and J. E. Mooij, Phys. Rev. B **35**, R7291 (1987).

[10] H. S. J. van der Zant, W. J. Elion, L. J. Geerligs, and J. E. Mooij, Phys. Rev. B **54**, 10081 (1996).

[11] S. Chakravarty, G. L. Ingold, S. Kivelson, and A. Luther, Phys. Rev. Lett. **56**, 2303 (1986); S. Chakravarty, G. L. Ingold, S. Kivelson, and G. Zimányi, Phys. Rev. B **37**, 3283 (1988).

[12] M. P. A. Fisher, Phys. Rev. Lett. **57**, 885 (1986); S. Chakravarty, S. Kivelson, G. T. Zimányi, and B. I. Halperin, Phys. Rev. B **35**, R7256 (1987).

[13] E. Šimánek and R. Brown, Phys. Rev. B **34**, R3495 (1986).

[14] U. Eckern, G. Schön and V. Ambegaokar, Phys. Rev. B **30**, 6419 (1984).

[15] A. Kampf, G. Schön, Physica **152**, 239 (1988); A. Kampf, G. Schön, Phys. Rev. B **36**, 3651 (1987); E. Šimánek and R. Brown, Phys. Rev. B **34**, R3495 (1986).

[16] J. Choi and J. V. José, Phys. Rev. Lett. **62**, 1904 (1989).

[17] A. J. Rimberg, T. R. Ho, Ç. Kurdak, J. Clarke, K. L. Campman, A. C. Gossard, Phys. Rev. Lett. **78**, 2632 (1997).

[18] Y. Takahide, R. Yagi, A. Kanda, Y. Ootuka and S. Kobayashi, Phys. Rev. Lett. **85**, 1974 (2000).

[19] A. Yazdani and A. Kapitulnik, Phys. Rev. Lett. **74**, 3037 (1995).

[20] A. D. Zaikin, Physica B **152**, 251 (1988).

[21] A. Cuccoli, A. Fubini, and V. Tognetti, R. Vaia, Phys. Rev. B **61**, 11289 (2000).

[22] T. P. Polak, T. K. Kopeć, Phys. Rev. B **72**, 014509 (2005).

[23] K.-H. Wagenblast, A. van Otterlo, G. Schön, and G. T. Zimányi, Phys. Rev. Lett. **78**, 1779 (1997).

[24] K.-H. Wagenblast, A. van Otterlo, G. Schön, and G. T. Zimányi, Phys. Rev. Lett. **79**, 2730 (1997).

[25] R. Yagi, T. Yamaguchi, H. Kazawa, S. I. Kobayashi, Physica **B** 227, 232 (1996).

[26] Y. Takahide, R. Yagi, A. Kanda, Y. Ootuka, S. I. Kobayashi,Phys. Rev. Lett. **85**, 1974 (2000).

[27] T. Yamaguchi, R. Yagi, A. Kanda, Y. Ootuka, S. I. Kobayashi, Physica **C** 352, 181 (2001).

[28] Y. Ootuka, Y. Takahide , H. Miyazaki , A. Kanda, Microelectronic Engineering 63, 30931 (2002).

[29] J. S. Penttilä, P. J. Hakonen, M. A. Paalanen, Ü. Parts, E. B. Sonin, Physica **B** 284, 1832 (2000).

[30] R. Fazio and G. Schön, Phys. Rev. B **43**, 5307 (1991).

[31] T. K. Kopeć and J. V. José, Phys. Rev. B **60**, 7473 (1999).

[32] M. Abramovitz and I. Stegun, *Handbook of Mathematical Functions* (Dover, New York, 1970).

[33] M. P. A. Fisher, Phys. Rev. B **36**, 1917 (1987).